



# Atmospheric Correction for Soil Information Extraction on AVIRIS Data

Luciano J. de O. Accioly & Alfredo R. Huete

EMBRAPA, Brazil and UNIVERSITY OF ARIZONA, USA

## Abstract

Land information from an airborne or spaceborne sensor is affected by atmosphere components. Atmospheric effects varies with time, space, wavelength, and target characteristics. The objective of this work was to compare the soil information content in spectra collected from soil samples, atmospherically corrected, and normalized radiances (apparent reflectances) from AVIRIS data. The data were collected from six soil series located at the Walnut Gulch Experimental Watershed – Arizona, for 0.45 to 0.90  $\mu\text{m}$ . Atmospheric model MODTRAN was used to generate apparent reflectances while the ATmosphere REMoval Program (ATREM) was utilized to extract soil ground reflectances. Both models were used for midlatitude, summer, rural continental visibility. Good agreement was found between atmospherically corrected AVIRIS data and ground reflectances for a calibration site with some overcorrection for water and ozone absorption bands. Soil spectral curves from apparent reflectances showed highly dependent on the soil brightness and this dependence varied with the wavelength. Iron affected soils were more affected by the influence of molecular scattering.

## INTRODUCTION

Information extraction of land target from airborne and spaceborne sensors is affected by the interactions of the income spectral solar irradiance and the target's spectral reflected energy with the components of the atmosphere. Scattering of solar energy by atmospheric molecules and particulates and absorption by atmospheric gaseous are responsible for the atmospheric noise on the land signal received by an airborne or spaceborne sensor. Molecular scattering (Rayleigh) is strongly wavelength dependent, being stronger at shorter wavelengths. Thus the upward "path radiance" created by the atmospheric scattering is higher in the blue region of the electromagnetic spectrum than in other parts of the visible and near infrared. The influence of the path radiance is also dependent of the sun/sensor viewing geometry and the reflectance characteristics of the target. As a result of these influences spectral features that help in discriminating soil types can be misinterpreted. The multiplicative and additive effects of atmospheric attenuation and scattering as well as the initial shape of the solar spectrum can be determined using a model of radiative transfer. The objective of this work was to compare the soil information content in spectra collected from soil samples, atmospherically corrected AVIRIS data, and normalized radiances (apparent reflectances) from AVIRIS data.

## METHODOLOGY

The study site is located within the Walnut Gulch Experimental Watershed, Tombstone, Arizona. The area of the Watershed imaged by AVIRIS is dominated by six soil series: McAllister, Stronghold, Graham, Tombstone, Baboquivari and Epitaph. When considering the parent material, some of the major soils in this Watershed such as Stronghold and Tombstone were largely influenced by the presence of limestone, while other, such as Baboquivari and McAllister have as their parent material m

993). The instrument operates in the 0.4-2.45  $\mu\text{m}$  region collecting 224 channels with a nominal spectral bandpass of 10 nm and a nominal spatial resolution of 20 m at a flight height of 20,000 m. AVIRIS data were collected over the study area on May 14, 1991 (dry season). The original AVIRIS image came as a scaled radiance image and was processed to continental surface reflectance imagery by using the Atmosphere Removal Program (ATREM) (Gao et al., 1996).

The interactions of incoming solar irradiance with the atmosphere and the surface has been described by Moran et al. (1992) using the following equation:

$$\Delta_{g8} = [B(L_{s8} - L_{d8}) / \vartheta_{-8}] / [(E_{08})\cos 2_z \vartheta_{z8} + E_{d8}9] \quad (1)$$

Where:

$\Delta_{g8}$  = spectral reflectance of the surface, after discounting the effects of atmospheric scattering and absorption;

$L_{s8}$  = spectral radiance at the satellite sensor ( $\text{Wcm}^{-2}\text{sr}^{-1} \mu\text{m}^{-1}$ );

$E_{d8}9$  = downwelling spectral irradiance at the surface due to scattered solar flux in the in the atmosphere ( $\text{Wcm}^{-2} \mu\text{m}^{-1}$ );

$L_{d8}8$  = upwelling atmospheric spectral radiance scattered in the direction of and at the sensor entrance pupil and within the sensor's field of view (spectral path radiance) ( $\text{Wcm}^{-2}\text{sr}^{-1} \mu\text{m}^{-1}$ );

$\vartheta_{z8}$  = atmospheric spectral transmittance along the path from the sun to the ground surface where

$\vartheta_{z8} = \exp(-\tau_{z8})$  for scattering and weak absorption;

$\vartheta_{-8}$  = atmospheric spectral transmittance along the path from the ground surface to the sensor, where

$\vartheta_{-8} = \exp(-\tau_{-8})$  for scattering and weak absorption;

\* $\tau_{\lambda}$  = spectral extinction optical depth;

$E_{0\lambda}$  = solar spectral irradiance on a surface perpendicular to the sun's rays outside the atmosphere ( $Wcm^{-2}\mu m^{-1}$ );

$2_z$  = angle of incidence of the direct solar flux onto the earth's surface;

$2_c$  = angle between the line from the sensor to the surface and the normal to the surface of interest

$\lambda$  = spectral band.

Variation in at-sensor radiances can be reduced greatly by normalizing the radiance signal by the exo-atmospheric solar irradiance, i.e., by expressing the radiances in reflectance units known as apparent reflectance (Huete, 1996). Thus, the first approach used to calibrate the AVIRIS scene to reflectance was the apparent reflectance ( $\Delta_{g\lambda}$ ) defined by Moran et al. (1992) as:

$$\Delta_{g\lambda} = BL_{s\lambda} / (E_{0\lambda} \cos 2_z) \quad (2)$$

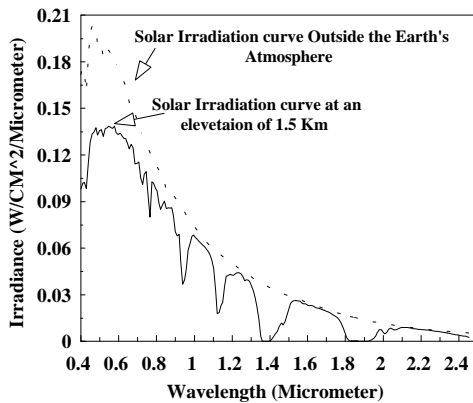
Where:

$L_{s\lambda}$  is the spectral radiance at the sensor ( $Wcm^{-2}sr^{-1}\mu m^{-1}$ );

$\Delta$  signifies uncorrected (or apparent) reflectance.

The solar spectral irradiance ( $E_{0\lambda}$ ) was given by the MODTRAN radiative transfer code for the transmittance mode (Berk et al., 1989) which also accounted for the solar-illumination geometry by using the latitude, longitude, and time of the AVIRIS data acquisition over the Walnut Gulch Watershed. MODTRAN was used for a midlatitude, summer, and rural (23 Km visibility) model based on the location and season of AVIRIS data acquisition. A plot of the irradiance values at the top of the Earth's atmosphere, as well as for the 1.5 Km altitude (average for the AVIRIS scene), as a function of the wavelength of the 210 nominal AVIRIS bands for this model is presented in Figure 1.

Figure 1 – Irradiance at the top of Earth's atmosphere and for 1.5 Km elevation as modeled by MODTRAN and convolved to AVIRIS bands



To extract ground reflectance the ATmosphre REMoval Program (ATREM) (Gao et al., 1996) was used. ATREM software derives scaled surface reflectance using an approximate atmospheric radiative transfer model (Gao et al., 1996). The program assumes horizontal surfaces that have lambertian reflectance. The atmospheric scattering effects are modeled in ATREM by using the Simulation of the Satellite Signal in the Solar Spectrum (5S) code (Tanre et al., 1986) with a user selected aerosol model. The transmittances of seven gases are calculated based on an assumed atmospheric model, the solar and observational geometries, and the Malkmus narrow band spectral model (Gao et al., 1996). For six gases ( $CO_2$ ,  $O_3$ ,  $N_2O$ ,  $CO$ ,  $CH_4$ , and  $O_2$ ), the algorithm assumes that the amount of gases are uniform across the scene. Only one transmittance spectrum is calculated for each of these gases (Gao et al., 1996). ATREM's algorithm treats the atmospheric water vapor differently. The algorithm derives water vapor values from AVIRIS data in the 0.94  $\mu m$  and 1.4  $\mu m$  regions on a pixel by pixel basis using a 3-channel ratioing technique and a look-up table procedure (Gao et al., 1996). An average value of 4,600 feet (1,550 m) for the elevation in the AVIRIS scene was used as input for the ATREM model. The channel ratio parameter was set for the default for soil rocks and minerals. It was also

used the aerosol continental model with a visibility of 50 km and 10 nm for output data resolution

Soil samples were collected from the first centimeter in depth from each one of the 6 most important soil series present in the AVIRIS scene. The air dry samples were crushed to pass through a 2 mm sieve before BRF measurements. The BRF was measured with the Spectron SE590 spectroradiometer (0.45-0.90  $\mu m$  spectral range in 0.01  $\mu m$  or 10 nm sampling interval). The soil samples were put in black plates 2 cm deep and 22 cm in diameter. The measurements were made outdoor on cloudless days. The outgoing radiance was collected with the sensor in the nadir view angle, while the solar zenith angle was about 30 degree. Reflectance factors were obtained by ratioing the reflected response from a soil by that of the spectralon panel with reflectance values adjusted for the sun angle.

To check the results of applying ATREM, one of the few "pure" targets found in the AVIRIS scene was selected. Subsurface horizons of the McAllister soil series were exposed after removal of surface horizon. This target had virtually no vegetation and represented an area of about 4 x 5 AVIRIS pixels. The four pixel in the center of this area (UTM coordinates of the upper left corner pixel: 3510400 N, and 592443 W, zone 12) were selected for making measurements with the Spectron SE590 instrument.

All spectral curves obtained with the Spectron instrument were convolved using a Gaussian filter in order to match the AVIRIS spectral bands.

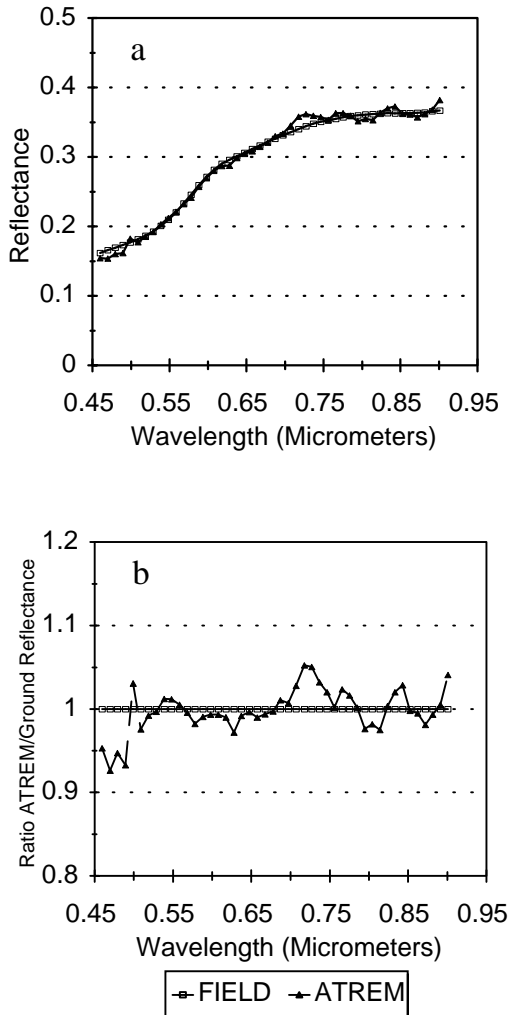
## RESULTS AND DISCUSSION

Figure 2 presents a comparison between ground reflectance values obtained for the "pure" target with AVIRIS reflectance values for the same target. The calibration of AVIRIS data with ATREM code presented a good fit for the measured spectral range (0.45 - 0.90  $\mu m$ ). The good agreement of ATREM code can be better interpreted by the ratio according to the wavelength of ATREM and the measured ground reflectance presented in Figure 2b. The results shows

that for this spectral range the deviation of ATREM from the measured field spectra range from -7.% (ratio of 0.93) to 5% (ratio of 1.05). The greater deviations are due to ATREM's overcorrectio

oil but also from other types of materials such green and yellow vegetation and litter mixed in different proportions.

Figure 2 – Calibration results of AVIRIS data with ATREM radiative transfer code



ATREM was believed to better remove the remains of water vapor, however, other authors (Verdebut et al.,1993; Huete, 1996) report the same characteristic peaks in the NIR region in spectra extracted from bare soil and brown fields and pointed out that a slight error in the wavelength calibration file can cause such small disturbance in the ATREM spectral curves. Apparent reflectance curves presented higher values for blue and green regions than ATREM radiative transfer code. The highest difference was found in 0.46  $\mu\text{m}$  with an increase in relation to ATREM's results that varied from 21% for Stronghold to 60% for Epitaph. The increase in reflectance values for the extreme portion of the short wavelengths was caused mainly by the great contribution of molecular scattering in this portion of the spectrum which was not removed by using apparent reflectance. The presence of molecular scattering in apparent reflectance curves tended to reduce the spectral differences between soil series, mostly in the blue region of the spectrum. Those differences were reduced because the contribution of molecular scattering was not the same for bright and dark target. Thus, for Epitaph soil series, which had very low values of reflectance in the blue region, the contribution of molecular scattering can reach values 60% over ATREM's results, while Stronghold, which have relatively high values for reflectance in the blue region, this contribution is at most 21% of ATREM's results. Soil spectral information was also reduced as a result of the influence of molecular scattering on apparent reflectance. One example of losing information was related to iron and iron-oxide content in soils which presented a decrease in reflectance values in the blue region of the spectrum as the iron content increased (Irons et al., 1989). Thus, McAllister soil which has spectral absorption feature in the blue region due to the higher iron-oxide content was more affected by the molecular scattering than the other soils. From about 0.54  $\mu\text{m}$  the reflectance values for apparent reflectance became less than that found for ATREM for most of the soils. However, for dark soils, such as Epitaph, values of apparent reflectance remained higher than that found for radiative transfer codes for longer wavelengths. Compared to ATREM,

the reduction in apparent reflectance values for wavelengths longer than 0.54  $\mu\text{m}$  (excluding regions more affected by water absorption bands) was higher for brighter soils (McAllister and Stronghold) than for dark soils (Epitaph). Moran et al. (1990), found that the apparent reflectance taken on a fallow field by the HRV sensor (mounted in SPOT-1 satellite) tended to overestimate surface reflectance in band XS1 (0.50 - 0.59  $\mu\text{m}$ ) and underestimate in band XS3 (0.79 - 0.89  $\mu\text{m}$ ). However for band XS2, located in the interval of 0.61 - 0.68  $\mu\text{m}$ , Moran et al. (1990) found that apparent reflectance was either underestimated or overestimated, illustrating the interplay of path radiance and atmospheric radiance as a function of reflectance. These results agreed with Huete (1996) who found that soil spectral signatures that were contaminated with atmosphere tended to present higher blue and green responses and were attenuated by gas absorption, particularly the secondary water vapor absorption bands, such as at 0.92 and 0.83  $\mu\text{m}$ , and by the oxygen band near 0.76  $\mu\text{m}$ .

**CONCLUSIONS**

Overcorrection of water and ozone absorption bands affected the ATREM's calibration results for soil information extraction from AVIRIS data. The results were also affected by the presence of components other than soils in a single pixel. Soil spectral curves from apparent reflectance showed highly dependence on the soil brightness and this dependence varies with the wavelength. Iron affected soils, such as McAllister, were more affected by the influence of molecular scattering on apparent reflectances in the blue region of the spectrum.

**REFERENCES**

Berk, A., L.S. Bernstein, and D.C. Roberson. 1989. MODTRAN: A moderate Resolution Model for LOWTRAN 7. U.S. Air Force Geophysical Laboratory (AFGL), Hanscom Air Force Base, Massachusetts

Gao, B.C., K.B. Heidebrecht, and A.F.H. Goetz. 1996. Atmospheric Removal Program (ATREM)Users Guide, Centre for the Study of Earth from Space, Cooperative Institute for Research in Environmental Sciences, University of Colorado, Boulder.

Huete, A.R. 1996. Extension of soil spectra to the satellite: Atmosphere, geometric, and sensor considerations. *Photo-Interpretation* 2:101-114.

Irons, J.R., R.A. Weismiller, G.W. Petersen. 1989. Soil Reflectance. p.66-106. In: Asrar, G. (ed.) *Theory and Applications of Optical Remote Sensing*. John Wiley & Sons, NY.

Moran, M.S., R.D. Jackson, P.N. Slater, and P.M. Teillet, 1992. Evaluation of simplified procedures for retrieval of land surface reflectance factors from satellite sensor output. *Remote Sens. Environ.* 41:169-184.

Moran, M.S., R.D. Jackson, G.F. Hart, P.N. Slater, R.J. Bartell, S.F. Biggar, D.I. Gellmand, and R.P. Santer. 1990. Obtaining surface reflectance factors from atmospheric and view angle corrected SPOT-1 HRV data. *Remote Sens. Environ.* 32:203-214.

Tanre, D., C. Derro, P. Duhaut, M.Herman, J.J.Morcrette, J.Perbos, and P.Y.Deschamps. 1986. *Simulation of the Satellite Signal in the Solar Spectrum (5S), User's Guide* (U.S.T. de Lille, 59655 Villeneuve d'ascq, France: Laboratoire d'Optique Atmospherique).

Vane, G., Duval, J.E., and Wellman, J.B. 1993. *Imaging spectroscopy of the Earth and other solar*

system bodies. p. 121-143. In Pieters, C.M., and P.A Englert., (ed.) *Remote Geochemical Analysis: Elemental and Mineralogical Composition*. Cambridge University Press, New York.

Verdebut, J., G. Schmuck, S.L., Ustin, S.J. Sieber. 1993. Multitemporal AVIRIS-images of forested and agricultural units in southern Germany. p.23-31. In: Vane, G.(ed.) *Imaging Spectrometry of the Terrestrial Environment. Proceedings of The International Society for Optical Engineering (SPIE), Orlando, Fl. 14-15 April, 1993.*

Figure 3 – Comparisson between soil spectra obtained from AVIRIS (ATREM and apparent reflectance) data and lab data

